Surg Radiol Anat (2015) 37:1217–1224
DOI 10.1007/s00276-015-1511-y

ORIGINAL ARTICLE

Morphometric study of the greater palatine canal: cone-beam computed tomography

O. Rapado-González[1] · J. A. Suárez-Quintanilla[2] · X. L. Otero-Cepeda[3] · A. Fernández-Alonso[1] · M. M. Suárez-Cunqueiro[1]

Received: 28 January 2015 / Accepted: 11 June 2015 / Published online: 24 June 2015

Abstract
Purpose To analyze greater palatine canal (GPC) dimensions using cone-beam computed tomography (CBCT) images, and to evaluate the position of the greater palatine foramen (GPF) with respect to various landmarks selected in relation to dental status.
Methods This study included 150 CBCTs. Axial slices were used to determine the position and dimensions of the GPF. Sagittal slices were used to assess GPC length. Reference lines were established to evaluate the GPC diameter in sagittal and coronal slices.
Results From the 77 GPF analyzed, 76 were located on level 2. Average posterior GPF distance was 6.59 ± 3.27 mm on right side and 7.35 ± 3.40 mm on left side. Several measurements to determine the position and dimensions of the GPF presented significant values ($p \leq 0.05$). GPC length was 12.31 ± 1.96 mm on right side and 12.52 ± 2.15 mm on left side, statistically significant differences were detected between genders only on right canal ($p \leq 0.004$). Sagittal and coronal reference lines presented significantly higher values for men except for the S3 ($p < 0.062$) and C1 ($p < 0.067$) in the left GPC.
Conclusions CBCT is a useful tool for evaluating GPC morphometrically in the three anatomical slices. The sagittal nasal plane and posterior nasal plane are two intraoral anatomical landmarks for the location of the GPF. Their scant variability allows accurate identification of GPFs in both dentate as well as edentulous patients.

Keywords Greater palatine canal · Greater palatine foramen · Cone-beam computed tomography · Upper jaw · Pterygopalatine fossa

Introduction

The pterygopalatine fossa is an anatomic structure with morphology in inverse pyramid that is connected to the oral cavity by the greater palatine canal (GPC) [7]. The vascular-nervous package consisting of the maxillary nerve, accompanied by the maxillary artery, venous rami and pterygopalatine ganglion is located in the interior of this fossa [3]. The maxillary nerve enters the pterygopalatine fossa from the trigeminal ganglion through the round foramen. The maxillary nerve joins the Meckel sphenopalatine ganglion through small nervous rami, and then the greater and lesser palatine nerves arise. The greater palatine nerve emerges on the palate through the greater palatine foramen (GPF) and the lesser palatine nerves emerge through their corresponding foramina [9, 20].

The position of the GPF in the bony surface of the palate is of great interest to dentists, maxillofacial surgeons and otolaryngologists for anesthetic purposes as well as the harvesting of subepithelial connective tissue grafts [10]. The GPF is hidden by thick mucous, and therefore, it is important to determine its clinical location with respect to anatomical landmarks [8, 26]. Various skull studies [4, 19, 21, 23] have analyzed the position of the GPF, but studies involving cone-beam computed tomography (CBCT) are scarce [12].

✉ M. M. Suárez-Cunqueiro
mariamercedes.suarez@usc.es

[1] Department of Stomatology, Medicine and Dentistry School, University of Santiago de Compostela, C/Entrerrios S/N, 15872 Santiago de Compostela, Spain

[2] Department of Anatomy, Medicine and Dentistry School, University of Santiago de Compostela, A Coruña, Spain

[3] Biostatistical Department, Medicine and Dentistry School, University of Santiago de Compostela, A Coruña, Spain

Anesthesia applied through the GPC affects the maxillary teeth, palate and gingival tissue, half face skin, nasal cavity and sinuses [10]. A thorough knowledge of the GPC is necessary to avoid clinical complications [16, 18, 29] affecting the vascular and nervous structures in the pterygopalatine fossa. To the best of our knowledge, no previous CBCT studies exist that analyze the GPC on the three anatomical slices. CBCT images can be seen in the three orthogonal planes at the same time.

The purpose of the present study is twofold. First, to analyze GPC dimensions using CBCT images, and, second, to evaluate the position of the GPF with respect to various landmarks selected in relation to dental status.

Materials and methods

Our overall sample consisted of 1551 consecutive CBCTs pertaining to patients referred to the Radiology Unit of the Medicine and Dentistry School at the University of Santiago de Compostela. CBCTs were performed from July 2008 to March 2012 for treatment planning of various oral surgical procedures. A total of 187 CBCTs were selected randomly. All CBCTs were classified according to dental status into one of three groups: dentate (G1), with both premolars and first upper molar bilaterally; partially edentulous (G2), unilateral or bilateral absence of premolars or first upper molar; or total edentulous (G3), absence of teeth in upper jaw arch. This study was approved by the Galician Ethics Committee of Clinical Research (Ref: 2012/272). Written informed consent was obtained from all patients to participate in the study.

The inclusion criteria were the following: (1) patients aged 18 years or older; and (2) CBCTs with voxel size of 0.3 mm or less. The exclusion criteria were: (1) trauma, (2) craniofacial surgery, (3) orthognathic surgery, (4) bony pathology in the upper jaw, (5) absence of the GPF, (6) ossification of the GPC, (7) dental implants in the alveolar region of premolars and molars, (8) artifacts in the region of interest or (9) CBCTs that do not include the upper jaw.

Image evaluation

CBCTs were done using a 17-19 i-CAT scanner (Imaging Sciences International, Inc., Hatfield, Pennsylvania, USA) (5 mA, 120 kVp, 14.7 s) and evaluated by an experienced graduate student. Analysis was carried out using i-CATVision software (i-CATVision 1.9, Imaging Sciences International, Inc., Hatfield, Pennsylvania, USA). CBCT slice thickness was 0.25 mm.

All measures were taken for GPF and GPC on both sides in each CBCT. Axial slices were used to assess GPF position and dimensions. GPC length and reference lines were analyzed in the sagittal and coronal slices.

Measurements to determine the position and dimensions of the GPF

The following landmarks were selected to standardize measurements on the axial slices: (1) GPF–PNP was defined as the perpendicular distance from the posterior edge of the GPF to posterior nasal plane (PNP). The PNP is the most posterior anatomical plane of the posterior nasal spine (PNS); (2) GPF–ANS was calculated drawing a line from the anterior nasal spine (ANS) to the anterior edge of the GPF; (3) ANS–PNP was obtained by drawing a perpendicular line to the PNP from the most anterior point of the ANS and represents the sagittal nasal plane (SNP); (4) GPF–SNP was defined as the distance from the anterior edge of the GPF to SNP; (5) GPF–BBP was calculated as the distance from the medial edge of the GPF to the buccal bone plate (BBP); (6) anterior nasal angle (ANA) was evaluated by joining ANS–GPF distances; (7) posterior nasal angle (PNA) was assessed by drawing a line from the PNP to the anterior edge of the GPF; (8) GPF width was calculated in the anterior–posterior direction (Dap) (joining the most anterior and posterior concavity of GPF) and transverse direction (Dt) (joining the most mesial and distal concavity of GPF) (Fig. 1).

Position of GPF in relation to first upper molar

Evaluation of GPF position with respect to first upper molar was carried out only on sides that also presented the

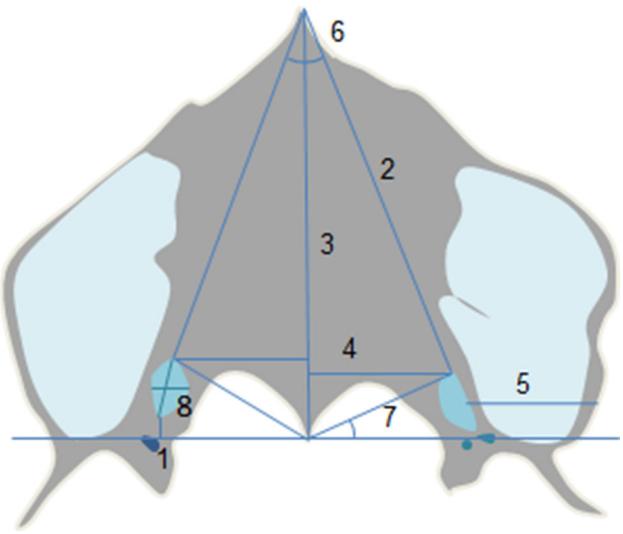

Fig. 1 Landmarks selected to determine the position and dimensions of the GPF in axial image: *1* GPF–PNP, *2* GPF–ANS, *3* ANS–PNP, *4* GPF–SNP, *5* GPF–BBP, *6* ANA, *7* PNA and *8* GPF width

first and second premolar. The position of the GPF was determined by drawing a line from the distal aspect of the maxillary first molar in the interdental space perpendicular to the median palatine suture. To determine the GPF distance, a perpendicular line was drawn from the anterior edge of the GPF to the interdental line. The GPFs touching the interdental line were denominated level 0. Those located in the anterior region of the interdental line were denominated level 1 and those in the posterior area were denominated level 2. The anterior GPF distances were represented by negative values and posterior GPF distances by positive values (Fig. 2).

Measurements to determine GPC length and reference lines

In order to standardize measurements, reference lines were established on the sagittal slice to measure the anterior–posterior diameter of the GPC. The upper line was drawn at the lower limit of the pterygopalatine fossa, and the lower line was located at the lower end of the palatine canal connecting the anterior and posterior walls. A third reference line was established at the midpoint between these two lines. These sagittal reference lines were named for their location on the canal: S1 (represents the diameter in the lower portion of the pterygopalatine fossa), S2 (represents the diameter in the middle of the GPC) and S3 (represents the maximum diameter at the lower end of the palatine canal) (Fig. 3).

The length of the GPC was measured by determining the distance between the upper and lower sagittal reference lines.

The three sagittal reference lines were used as landmarks to measure the transverse diameter of the canal in the coronal slices. For this, the axial cursor was located on each reference line and the coronal cursor was located perpendicular to the axial cursor. Thus, we established three new coronal reference lines for the transverse diameter of the canal. These coronal reference lines were named for their location on the canal: C1 (represents the diameter in the lower portion of the pterygopalatine fossa); C2 (represents the diameter in the middle of the GPC) and C3 (represents the maximum diameter at the lower end of the palatine canal) (Fig. 4). In terms of the spatial position in the canal, both sagittal and coronal reference lines are homologous. Thus, S1 determined C1, S2 determined C2 and S3 determined C3.

Statistical analysis

Analyses were performed using SPSS 15.0 software for Windows (SPSS, Chicago, IL, USA). The mean value, standard deviation (SD), minimum value and the maximum value of the variables in the study are presented in the tables. The adjustment to the normal distribution was tested by the Kolmogorov–Smirnov test. Comparisons of mean values between men and women were performed using the Student's *t* test for independent samples. ANOVA contrasts were applied for comparisons between dental groups (G1, G2 and G3) and posteriori comparisons were made with the Bonferroni method. The coefficient of determination (R^2) was calculated to measure the degree of correlation between variables, and finally, multivariate linear regression models (MLRM) were applied to construct a prediction model of GPF values depending on the values of correlated variables. Statistical significance was set at $p \leq 0.05$. To check the intraobserver variability, Kappa test for the levels of GPF position and the intraclass correlation coefficient for the GPF and GPC measurements were used in 20 CBCTs.

Results

A total of 150 CBCTs were included in the study. Thirty seven CBCTs (out of 187) were not included due to the following reasons: poor image quality, implants in

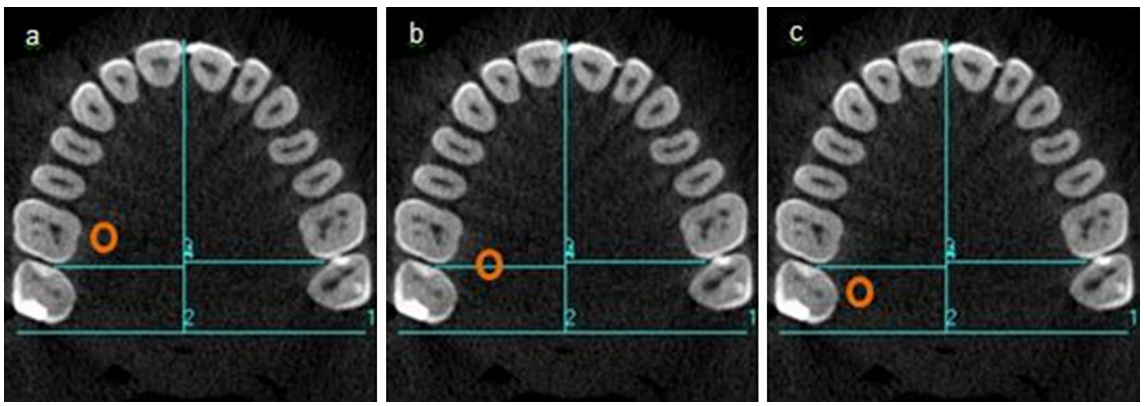

Fig. 2 Representation of the three levels GPF position. **a** Level 1, **b** level 0, **c** level 2

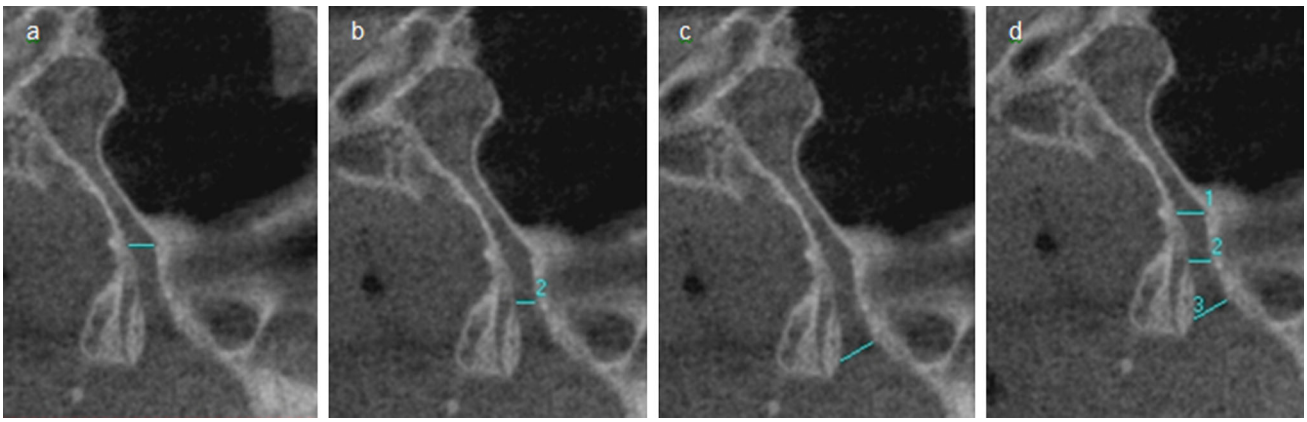

Fig. 3 Sagittal *reference lines*. **a** S1; **b** S2; **c** S3; **d** S1, S2 and S3

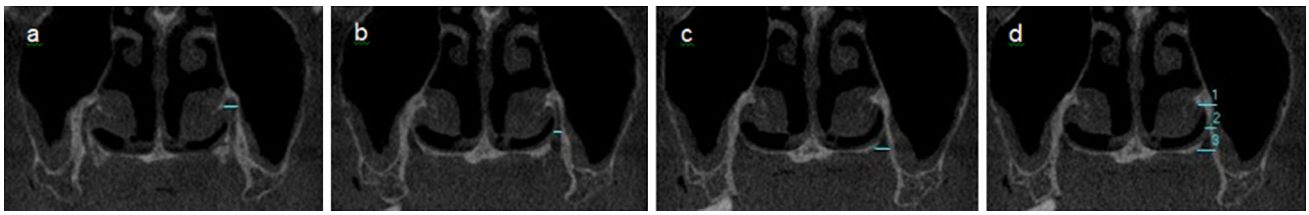

Fig. 4 Coronal *reference lines*. **a** C1; **b** C2; **c** C3; **d** C1, C2 and C3

Table 1 Descriptive GPF measurements

Parameters		Mean	SD	Minimum	Maximum
GPF–PNP	GPF-R	3.63	1.91	0	8.40
	GPF-L	3.94	1.97	0	9.75
GPF–SNP	GPF-R	15.05	2.00	9.50	20.50
	GPF-L	15.44	1.98	6.00	19.80
GPF–ANS	GPF-R	46.90	3.24	39.14	55.29
	GPF-L	46.83	3.19	39.05	56.29
GPF–BBP	GPF-R	11.91	2.34	5.00	19.00
	GPF-L	12.35	2.59	5.25	19.75
Dap	GPF-R	6.04	1.18	3.64	9.46
	GPF-L	6.04	1.12	4.00	9.41
Dt	GPF-R	2.72	0.74	1.20	4.50
	GPF-L	2.64	0.75	1.00	4.50

GPF-R right GPF, *GPF-L* left GPF, *SD* standard deviation

anatomical study area or ossification of the GPC. The study group comprised 55 males (36.67 %) and 95 females (63.33 %). On average, the ANA (38.91° ± 4.04°) was greater than the right posterior nasal angle (ANP-R) (31.99° ± 7.47°) or the left posterior nasal angle (ANP-L) (32.16° ± 7.26°) (Tables 1, 2).

GPF location relative to the distal aspect of the maxillary first molar was evaluated in 38 right and 39 left foramina. All left GPF (GPF-L) were located on level 2. Of the right GPF (GPF-R), 37 were found at level 2 and one at level 0. None of the evaluated CBCTs showed GPFs at level 1. Average posterior GPF distance was lower on right side (6.59 ± 3.27 mm) as compared to left side (7.35 ± 3.40 mm).

Table 2 GPC length and diameters measured in the sagittal and coronal slices

Parameters		Mean	SD	Minimun	Maximum
GPC length	GPC-R	12.31	1.96	8.06	16.53
	GPC-L	12.52	2.15	8.14	17.34
Sagittal level					
S1	GPC-R	2.94	0.86	1.00	6.75
	GPC-L	2.90	0.90	1.00	5.50
S2	GPC-R	3.53	0.98	1.50	6.25
	GPC-L	3.61	0.97	1.50	7.07
S3	GPC-R	6.10	1.52	2.50	10.77
	GPC-L	6.27	1.70	3.05	11.96
Coronal level					
C1	GPC-R	2.16	0.52	1.00	3.75
	GPC-L	2.18	0.51	1.00	3.90
C2	GPC-R	2.01	0.50	1.00	3.75
	GPC-L	1.99	0.50	0.75	3.75
C3	GPC-R	3.76	1.11	1.75	6.75
	GPC-L	3.63	1.06	1.50	8.70

GPF-R right GPF, *GPF-L* left GPF, *SD* standard deviation

Table 3 Dimensions of GPF in relation to gender

Parameters	Right side					Left side			
	Gender	Mean	SD	*F*	*p*	Mean	SD	*F*	*p*
GPF–PNP	Female (f)	3.27	1.93	1.279	0.002*	3.69	1.98	0.001	0.042*
	Male (m)	4.27	1.73			4.37	1.90		
GPF–SNP	f	15.06	1.93	1.547	0.950	15.51	1.88	0.279	0.599
	m	15.04	2.15			15.33	2.16		
GPF–ANS	f	45.98	2.62	8.947	0.003*	45.94	2.78	1.524	<0.001*
	m	48.49	3.60			48.37	3.29		
GPF–BBP	f	11.61	2.22	0.851	0.042*	12.12	2.51	0.409	0.151
	m	12.41	2.48			12.75	2.71		
PNA	f	30.74	6.62	5.624	0.011*	30.99	6.69	0.032	0.009*
	m	34.16	8.38			34.18	3.88		
Dap	f	5.84	1.20	0.926	0.005*	5.86	1.03	2.435	0.011*
	m	6.39	1.07			6.33	1.21		
Dt	f	2.48	0.67	0.114	<0.001*	2.39	0.66	0.700	<0.001*
	m	3.14	0.67			3.06	0.72		

SD standard deviation

* Statistically significant differences $p < 0.05$

Table 4 Dimensions of GPC in relation to gender

	Right side					Left side			
	Gender	Mean	SD	*F*	*p*	Mean	SD	*F*	*p*
GPC length	Female (f)	11.97	2.02	3.136	0.004*	12.27	2.18	0.537	0.053
	Male (m)	12.91	1.70			12.97	2.05		
Sagittal level									
S1	f	2.71	0.70	5.625	<0.001*	2.73	0.85	1.534	0.002*
	m	3.33	0.98			3.19	0.92		
S2	f	3.26	0.86	2.718	<0.001*	3.38	0.85	1.467	<0.001*
	m	3.99	1.02			4.01	1.06		
S3	f	5.74	1.43	0.357	<0.001*	6.05	1.45	6.372	0.062
	m	6.71	1.51			6.64	2.03		
Coronal level									
C1	f	2.06	0.46	2.814	0.003*	2.12	0.49	0.269	0.067
	m	2.33	0.57			2.28	0.53		
C2	f	1.88	0.47	0.234	<0.001*	1.88	0.44	3.578	<0.001*
	m	2.22	0.50			2.19	0.55		
C3	f	3.47	1.03	0.044	<0.001*	3.30	0.87	1.961	<0.001*
	m	4.27	1.09			4.18	1.12		

SD standard deviation

* Statistically significant differences $p < 0.05$

In relation to gender, the dimensions of the GPF–PNP, GPF–ANS, PNA, Dap and Dt pertaining to both GPF sides presented significantly lower values in women. On the other hand, average ANS–PNP distance did present statistically significant ($p < 0.001$) differences, with a value of 52.71 ± 3.35 mm for women and 56.50 ± 3.96 mm for men. ANA was also found to be significantly different ($p < 0.009$) by gender. In women the average ANA was 39.57° ± 3.88° and in men the average was 37.78° ± 4.09°. Regarding GPF–SNP distance, we found no significant differences between genders. No statistically significant differences were observed between genders regarding GPF distance. However, GPF–BBP distance on the right side was statistically significant ($p < 0.042$) between women and men (Table 3).

With respect to GPC dimensions, the length of the canal was slightly greater in males, but this difference was only statistically significant in the right GPC (GPC-R).

Table 5 Effect of dental status on GPF–SNP, GPF–BBP and ANA dimensions

Parameters		Status dental	Status dental	*F*	*p*
GPF–SNP	GPF-L	G1	G2	6.776	0.002*
	GPF-R	G1	G2	10.437	<0.001*
GPF–BBP	GPF-L	G1	G3	6.405	0.002*
		G3	G2	6.405	0.036*
	GPF-R	G1	G3	8.468	<0.001*
		G1	G2	8.468	0.025*
		G3	G2	8.468	0.026*
ANA		G1	G2	10.539	0.002*

GPF-R right GPF, *GPF-L* left GPF, *G1* dentate group, *G2* partially edentulous group, *G3* total edentulous group, *SD* standard deviation

* Statistically significant differences $p < 0.05$

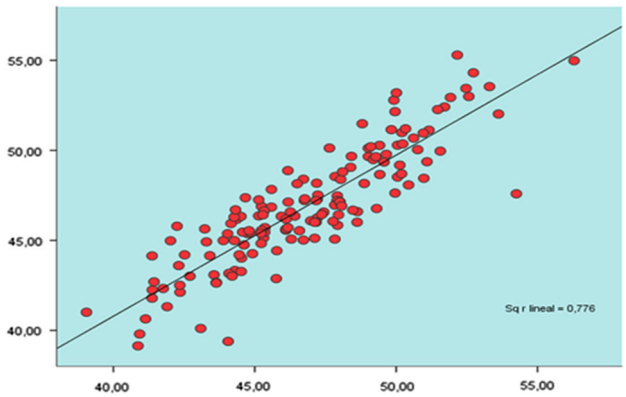

Fig. 5 *Scatterplot* of right and left GPF–ANS: *vertical axis* represents right GPF–ANS and *horizontal axis* represents left GPF–ANS

Regarding sagittal reference lines, S1, S2 and S3 presented significantly higher values for men, except for the S3 ($p < 0.062$) in the left GPC (GPC-L). Statistically higher values for men were also observed in all three coronal reference lines, except for C1 ($p < 0.067$) in the GPC-L (Table 4).

Statistically significant differences in both GPF-L and GPF-R were found by dental status groups. The parameters showing these differences were GPF–SNP distance, GPF–BBPA distance and ANA. G1 presented significantly different GPF–SNP distances as compared to G2. GPF–BBP distance in GPF-R was statistically different in all three dental status groups and in GPC-L was statistically different in two dental status groups. ANA dimensions were significantly different between groups G1 and G2 ($p < 0.002$) (Table 5).

Regarding degree of correlation GPF–BBP and GPF distance presented R^2 values of 0.64 and 0.65, respectively. The greatest degree of correlation between right and left sides was observed in GPF–ANS, where $R^2 = 0.776$ (Fig. 5).

MLRM were performed to show the degree of relationship of the variables PNA, ANS–PNP, GPF–ANS, GPF–SNP and Dap in the GPF–PNP distance. We found significant values in right side ($R^2 = 0.773$; $p < 0.001$) and left side ($R^2 = 0.746$; $p < 0.001$).

Intraobserver variability

With respect to levels of GPF position, the intraobserver variability was a Kappa value ranging from 0.49 to 0.58. And regarding the GPF and GPC measurements, the intraobserver variability was an intraclass correlation coefficient value ranging from 0.82 to 0.87.

Discussion

To the best of our knowledge, this is the first time an analysis has been carried out of GPC which establishes three reference lines in both the sagittal and coronal slices. A thorough understanding of the dimensions and location of GPC provides a more reliable view of the bone structure.

The GPC is located in an area of confluence of several anatomical structures and has great clinical relevance. Access and direct application of anesthesia to neurovascular content which is present in the pterygopalatine fossa achieves maxillary nerve block and allows for various surgical procedures in the palatal region. In addition, proper access to GPC is essential for diagnosis, management and therapeutic treatments of orofacial pain syndromes [19]. Three-dimensional understanding of GPF is useful for limiting the likelihood of iatrogenic damage, but this is made difficult by several factors.

The location of the GPF by touch is constrained by existing palatal mucosa thickness, mainly in mucosal biotypes of great consistency. The topographic study in relation to the dentition is limited primarily by the need to provide dentate posterior sectors. The use of teeth as a

landmark is unreliable due to positional changes that may occur. Moreover, this parameter would not be useful in cases of completely or partially edentulous patients. CBCT provides three-dimensional images that can identify bony landmarks, both for localization GPF with the highest degree of accuracy.

The present study found an average GPF–PNP distance similar to prior research [1, 4, 15, 17, 26]. In the study by Saralaya and Nayak [25] on an Indian population, the average GPF–PNP was 4.20 mm, which is similar to a European study by Nimigean et al. [21] and a Brazilian study by Urbano et al. [32]. However, using a sample of 105 skulls of Thai origin, Methathrathip et al. [19] obtained an average distance of 2.10 mm. Westmoreland and Blanton [35] obtained an even shorter average GPF–PNP of 1.90 mm. Conversely, longer average distances were found in a Korean study by Hwang et al. [11] and an Indian study by Dave et al. [5]. Small differences between GPF-R and GPF-L have been observed, although there is great variability among populations of the same and different ethnicity. In the present study, GPF–PNP distance was measured with respect to the PNP, the rearmost portion of the PNS, whereas other authors have analyzed the position of GPF with respect to the greatest concavity of the palate or to the side of the hard palate margin [31].

SNP is another easily identifiable clinical anatomical point. The average GPF–SNP distance observed in the present study differed slightly from various ethnic studies [4, 5, 19, 21, 22, 26, 31, 32]. In a sample of 50 CBCTs, Ikuta et al. [12] found a similar average distance to the present study, as did another European study by Piagkou et al. [23]. With respect to right and left side SNP differences, although we found little difference, the African study by Osunwake et al. [22] found a 0.70 mm discrepancy. Other authors with samples from Europe and Brazil found a discrepancy of 0.50 mm [22, 30, 31]. Symmetric growth of GPFs can be affected by sutural growth between the maxilla and the palatine bone and an increase in the length of the palate accompanied by tooth eruption [28, 31].

Another parameter that we have analyzed was GPF–BBP distance. Alterations in the width of the alveolar ridge may be due to physiological resorption with age, the use of full or partial prosthesis, traumatic extractions or alterations in bone metabolism [2, 13, 24, 33]. All these factors predispose morphological variations experienced by the alveolar crest, limiting the usefulness of BBP as a reference in locating the GPF. In particular, we do not recommend using BBP as a reference in edentulous patients, unlike other authors [12, 31].

In dentate patients, the position of the GPF has been determined with respect to multiple combinations of maxillary molars, yielding differences between study groups of the same ethnic origin and between populations of different geographical origin. Some authors [31] consider that the variability in the position of GPC is due to study design. Numerous researches have located the GPF opposite to the maxillary third molar in a high percentage [1, 4, 5, 12, 19, 21, 23, 25, 26, 31]. Few studies [14, 34] have observed GPFs with a position anterior to maxillary second molar. We found one GPF on level 0, but this position is infrequent. Many patients do not exhibit the maxillary second and third molar, so we have established a classification that may be useful in patients who only preserved the maxillary first molar.

In addition to the accurate position of GPF, it is important to know the dimensions of the GPC in order to apply anesthesia correctly. The average GPC length found in the present study was similar to some authors [11]; however, other authors such as Douglas et al. [6], Howard et al. [10] and Sheiki et al. [27] reported much greater lengths due to differences in study design. For example, Howard et al. [10] and Skeiki et al. [27] established the upper end of the GPC at the pterygoid canal, while we used the lower portion of pterygopalatine fossa.

Regarding the GPC reference lines in the sagittal and coronal slices, we found that the coronal transverse diameter was lower than the corresponding sagittal anterior–posterior diameter. The existence of diametrical variations in both sagittal and coronal slices could reflect intracanal tortuosity, thus limiting the distribution of morphological palatine neurovascular bundle.

Several authors have analyzed the Dap and Dt present in the GPF in the axial slice. The Indian study by Sharma and Garud [26] only assessed Dap with an average distance of 4.72 mm. Hwang et al. [11] used CT scans and found a similar Dap of 4.5 mm and a Dt of 2.20 mm. In the present study, using CBCT both diameters presented higher values.

Conclusion

We conclude that the CBCT is a useful tool for evaluating GPC morphometrically in the three anatomical slices. The SNP and PNP are two intraoral anatomical landmarks for the location of the GPF. Their scant variability allows accurate identification of GPFs in both dentate as well as edentulous patients.

Conflict of interest The authors declare that they have no conflict of interest.

Ethical standard This study complies with the current laws of Galicia (Spain) and it was approved by the Galician Ethics Committee of Clinical Research (Ref: 2012/272). Written informed consent was obtained from all patients to participate in the study.

References

1. Ajmani ML (1994) Anatomical variation in position of the greater palatine foramen in the adult human skull. J Anat 184:635–637
2. Chackartchi T, Stabholz A (2013) Ridge preservation after tooth extraction: what do we know today? Refuat Hapeh Vehashinayim 30:65–75
3. Chen CC, Chen ZX, Yang XD, Zheng JW, Li ZP, Huang F, Kong FZ, Zhang CS (2010) Comparative research of the thin transverse sectional anatomy and the multislice spiral CT on pterygopalatine fossa. Turk Neurosurg 20:151–158
4. Chrcanovic BR, Custódio AL (2010) Anatomical variation in the position of the greater palatine foramen. J Oral Sci 52:109–113
5. Dave MR, Yagain VK, Anadkat S (2013) A study of the anatomical variations in the position of the greater palatine foramen in adult human skulls and its clinical significance. Int J Morphol 31:578–583
6. Douglas R, Wormald PJ (2006) Pterygopalatine fossa infiltration through the greater palatine foramen: where to bend the needle. Laryngoscope 116:1255–1257
7. Erdogan N, Unur E, Baykara M (2003) CT anatomy of pterygopalatine fossa and its communications: a pictorial review. Comput Med Imaging Graph 27:481–487
8. Fu JH, Hasso DG, Yeh CY, Leong DJ, Chan HL, Wang HL (2011) The accuracy of identifying the greater palatine neurovascular bundle: a cadaver study. J Periodontol 82:1000–1006
9. Hawkins JM, Isen D (1998) Maxillary nerve block: the pterygopalatine canal approach. J Calif Dent Assoc 26:658–664
10. Howard-Swirzinski K, Edwards PC, Saini TS, Norton NS (2010) Length and geometric patterns of the greater palatine canal observed in cone beam computed tomography. Int J Dent. doi:10.1155/2010/292753
11. Hwang SH, Seo JH, Joo YH, Kim BG, Cho JH, Kang JM (2011) An anatomic study using three-dimensional reconstruction for pterygopalatine fossa infiltration via the greater palatine canal. Clin Anat 24:576–582
12. Ikuta CR, Cardoso CL, Ferreira-Júnior O, Pereira Lauris JR, Couto Souza PE, Fischer Rubira-Bullen IR (2013) Position of the greater palatine foramen: an anatomical study through cone beam computed tomography images. Surg Radiol Anat 35:837–842
13. Kawamoto S, Nagaoka E (2000) The effect of oestrogen deficiency on the alveolar bone resorption caused by traumatic occlusion. J Oral Rehabil 27:587–594
14. Klosek SK, Rungruang T (2009) Anatomical study of the greater palatine artery and related structures of the palatal vault: considerations for palate as the subepithelial connective tissue graft donor site. Surg Radiol Anat 31:245–250
15. Kumar A, Sharma A, Singh P (2011) Assessment of the relative location of greater palatine foramen in adult Indian skulls: consideration for maxillary nerve block. Eur J Anat 15:150–154
16. Leventhal D, Schwartz DN (2008) Infratemporal fossa abscess: complication of dental injection. Arch Otolaryngol Head Neck Surg 134:551–553
17. Lopes PTC, Santos AMPV, Pereira GAM, Oliveira VCBD (2011) Morphometric analysis of the greater palatine foramen in dry Southern Brazilian adult skulls. Int J Morphol 29:420–423
18. Mercuri LG (1979) Intraoral second division nerve block. Oral Surg Oral Med Oral Pathol 47:109–113
19. Methathrathip D, Apinhasmit W, Chompoopong S, Lertsirithong A, Ariyawatkul T, Sangvichien S (2005) Anatomy of greater palatine foramen and canal and pterygopalatine fossa in Thais: considerations for maxillary nerve block. Surg Radiol Anat 27:511–516
20. Norton NS (2007) Netter's head and neck anatomy for dentistry. Saunders, Philadelphia
21. Nimigean V, Nimigean VR, Buţincu L, Sălăvăstru DI, Podoleanu L (2013) Anatomical and clinical considerations regarding the greater palatine foramen. Rom J Morphol Embryol 54:779–783
22. Osunwoke EA, Amah-Tariah FS, Bob-Manuel IF, Nwankoala QK (2011) A study of the palatine foramen in dry human skulls in South-South Nigeria. Sci Afr 10:98–101
23. Piagkou M, Xanthos T, Anagnostopoulou S, Demesticha T, Kotsiomitis E, Piagkos G, Protogerou V, Lappas D, Skandalakis P, Johnson EO (2012) Anatomical variation and morphology in the position of the palatine foramina in adult human skulls from Greece. J Craniomaxillofac Surg 40:e206–e210. doi:10.1016/j.jcms.2011.10.011
24. Pietrokovski J (2013) The residual edentulous arches–foundation for implants and for removable dentures; some clinical considerations. A review of the literature 1954–2012. Refuat Hapeh Vehashinayim 30:14–24
25. Saralaya V, Nayak SR (2007) The relative position of the greater palatine foramen in dry Indian skulls. Singap Med J 48:1143–1146
26. Sharma NA, Garud RS (2013) Greater palatine foramen—key to successful hemimaxillary anaesthesia: a morphometric study and report of a rare aberration. Singap Med J 54:152–159
27. Sheikhi M, Zamaninaser A, Jalalian F (2013) Length and anatomic routes of the greater palatine canal as observed by cone beam computed tomography. Dent Res J (Isfahan) 10:155–161
28. Slavkin HC, Canter MR, Canter SR (1966) An anatomic study of the pterygomaxillary region in the craniums of infants and children. Oral Surg 21:225–235
29. Sved AM, Wong Head JD, Donkor P, Horan J, Rix L, Curtin J, Vickers R (1992) Complications associated with maxillary nerve block anaesthesia via the greater palatine canal. Aust Dent J 37:340–345
30. Teixeira CS, Souza VR, Maques CP, Silva Junior W, Pereira KF (2010) Topography of the greater palatine foramen in macerated skulls. J Morphol Sci 27:88–92
31. Tomaszewska IM, Tomaszewski KA, Kmiotek EK, Pena IZ, Urbanik A, Nowakowski M, Walocha JA (2014) Anatomical landmarks for the localization of the greater palatine foramen–a study of 1200 head CTs, 150 dry skulls, systematic review of literature and meta-analysis. J Anat 225:419–435
32. Urbano ES, Melo KA, Costa ST (2010) Morphologic study of the greater palatine canal. J Morphol Sci 27:102–104
33. Von Wowern N, Westergaard J, Kollerup G (2001) Bone mineral content and bone metabolism in young adults with severe periodontitis. J Clin Periodontol 28:583–588
34. Wang TM, Kuo KJ, Shih C, Ho LL, Liu JC (1988) Assessment of the relative locations of the greater palatine foramen in adult Chinese skulls. Acta Anat (Basel) 132:182–186
35. Westmoreland EE, Blanton PL (1982) An analysis of the variations in position of the greater palatine foramen in the adult human skull. Anat Rec 204:383–388